Adsorption Equilibria of *cis*-5,8,11,14,17-Eicosapentaenoic Acid Ethyl Ester and *cis*-4,7,10,13,16,19-Docosahexaenoic Acid Ethyl Ester on C18-Bonded Silica from Supercritical Carbon Dioxide

Baogen Su,[†] Huabin Xing,[†] Yisong Han,[†,‡] Yiwen Yang,[†] Qilong Ren,*[,†] and Pingdong Wu[†]

National Laboratory of Secondary Resources Chemical Engineering, Zhejiang University, Hangzhou 310027, China, and Hangzhou Hangyang Company Limited, Hangzhou 310004, China

The adsorption equilibrium of *cis*-5,8,11,14,17-eicosapentaenoic acid ethyl ester (EPA-EE) and *cis*-4,7,10,13,16,19-docosahexaenoic acid ethyl ester (DHA-EE) on C18-bonded silica from supercritical carbon dioxide was studied. The adsorption isotherms at (318.15, 328.15, and 338.15) K under pressures corresponding to carbon dioxide densities of (0.497, 0.618, and 0.723) $g \cdot mL^{-1}$ were determined by a static method. The isotherms were found to be of type II and could be well fitted by the BET equation. The monolayer adsorption amount of EPA-EE was (0.039 to 0.048) $mmol \cdot g^{-1}$, and that of DHA-EE was (0.040 to 0.063) $mmol \cdot g^{-1}$. At a given equilibrium molecular fraction of EPA-EE or DHA-EE in the bulk phase, the adsorption amount decreases slightly with temperature but decreases significantly with carbon dioxide density. Under the same conditions, the adsorption amount of DHA-EE is greater than that of EPA-EE. The adsorption isotherms of both EPA-EE and DHA-EE at different temperatures and carbon dioxide densities coincide to a general characteristic curve when they are plotted as a fractional monolayer coverage (q/q_m) vs reduced concentration (y/y_0). The isochoric heats of adsorption of EPA-EE and DHA-EE were in the range of (10 to 36) $kJ \cdot mol^{-1}$.

Introduction

cis-5,8,11,14,17-Eicosapentaenoic acid (EPA) and *cis*-4,7,10,13,16,19-docosahexaeonoic acid (DHA) have attracted great attention for their beneficial role in human health. These two ω-3 fatty acids are vital for the retina of the human eyes and the nervous system and can reduce the risk of cardiovascular disease and inflammatory disease as well.[1]

EPA and DHA are mainly produced from oils of marine fish such as tuna, sardine, and capelin. In the conventional process, the glycerides in fish oil are converted to ethyl esters (EE) or methyl esters (ME) of the fatty acids and then purified by solvent extraction, vacuum distillation, urea inclusion,[2] or HPLC.[3] To avoid toxic solvents and degradation under high temperature related to the conventional separation processes, separation of EPA-EE and DHA-EE by supercritical fluid chromatography (SFC) using supercritical dioxide ($SC-CO_2$) as the mobile phase has been studied recently.[3] Alkio et al.[5] prepared 95 % DHA-EE and 50 % EPA-EE at 338.15 K and 145 bar on C18-bonded silica (a silica gel surface modified with octadecyl groups). Yamaguchi et al.[6] used argentated silica gel as a stationary phase and acetone or acetonitrile as modifier to prepare 96 % DHA-EE. Pettinello et al.[7] prepared 90 % EPA-EE on silica gel. Yang et al.[8] found that EPA-EE could be separated from DHA-EE on silica gel or C18-bonded silica while other impurities were not well separated, and combination of the two stationary phases could improve the quality and productivity of EPA-EE and DHA-EE. A feasibility study[9] showed that a process using preparative SFC with CO_2 to produce pure EPA-EE from ethyl esterification products of fish oil could reduce the cost to about one-third of the conventional process.

Table 1. Physical Properties of C18-Bonded Silica

mean particle size	$5 \cdot 10^{-6}$ m
surface coverage	3.4 $\mu mol \cdot m^{-2}$
surface area	138.3 $m^2 \cdot g^{-1}$
pore volume	
< 30 Å	0.014 $cm^3 \cdot g^{-1}$
(30 to 200) Å	0.197 $cm^3 \cdot g^{-1}$
> 200 Å	0.014 $cm^3 \cdot g^{-1}$
average pore diameter	92.8 Å

Adsorption isotherms and related mathematical models of EPA-EE and DHA-EE are necessary for the optimization and engineering design of SFC separation. However, previous investigations on SFC separation of EPA-EE and DHA-EE have focused mainly on the operation technology. As a problem of

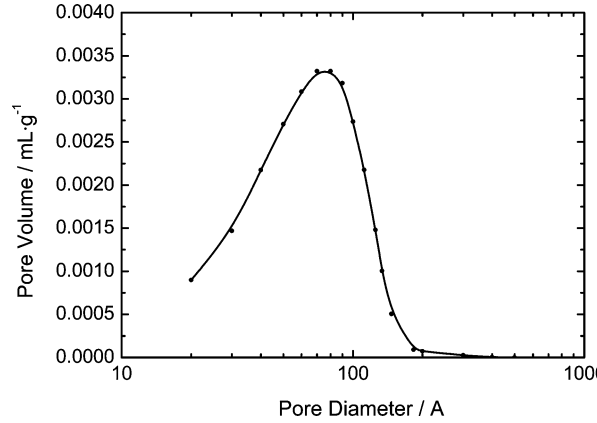

Figure 1. Pore size distribution of C18-bonded silica.

* To whom correspondence should be addressed. E-mail: renql@zju.edu.cn. Tel: +86 571 8795 2773. Fax: +86 571 8795 2773.
[†] Zhejiang University.
[‡] Hangzhou Hangyang Company Limited.

10.1021/je801003d CCC: $40.75
Published on Web 07/09/2009

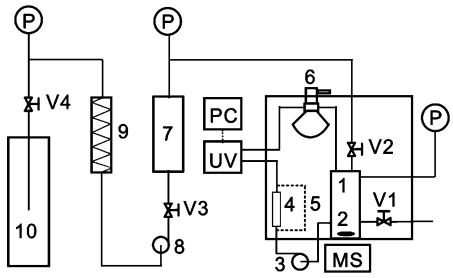

Figure 2. Schematic diagram of the adsorption apparatus. 1, mixing cell; 2, magnetic stirrer; 3, circulation pump; 4, adsorption column; 5, bypass tube; 6, six-port valve; 7, CO_2 reservoir; 8, CO_2 pump; 9, condenser; 10, CO_2 cylinder; 11, thermostat bath; V1,V2,V3,V4, stop valve; P, pressure gauge; UV, UV detector; PC, computer.

Table 2. Operation Temperatures and Pressures with Constant Densities

	P/MPa		
T/K	0.497 g·mL^{-1}	0.618 g·mL^{-1}	0.723 g·mL^{-1}
318.15	9.98	11.23	14.08
328.15	11.90	14.00	18.00
338.15	13.85	16.84	21.97

physical chemistry, adsorption of solute from supercritical fluids is of a unique nature in comparison with the adsorption from gas or common liquid solution. Up to now, the adsorption of only a few solutes from supercritical CO_2 has been studied in publications, such as toluene,[10,11] ethyl acetate,[10,11] tocopherol,[12−15] Vitamin D_3,[12,13] terpene,[16−18] furfural,[19] salicylic acid,[20] eicosane,[21] and some lipids.[22] In our previous work, adsorption isotherms of EPA-EE and DHA-EE on silica gel from supercritical CO_2 have been determined using the elution by the characteristic point (ECP) method.[1] It is well-known that the interaction between silica gel and the adsorbate is mainly due to the interaction between the polar hydroxyl group on the surface of silica gel and the adsorbate molecules. On the other hand, the interaction between C18-bonded silica and the adsorbate is based mainly on the dispersion force between C18 and the adsorbate molecules. To compare the adsorption characteristics of these two kinds of adsorbent, the present work was carried out by using C18-bonded silica. In addition, the ECP method is limited to very low concentration in the fluid phase so that the previous results were limited in the initial range of the isotherm, and the expected Langmuir isotherm was not well developed. In the present work, a better static method was used so that data at much higher concentration in the fluid phase could be obtained. As a result, adsorption data beyond the fluid phase concentration of the Langmuir isotherm were obtained. As a consequence, a relevant treatment of the data, different from the previous work, was used as well.

Experimental Section

Materials. Carbon dioxide with a purity of 99.995 % was purchased from the Hangzhou Minxing Gas Co. (Hangzhou, China); C18-bonded silica (5 μm) was purchased from EKA Chemical AB (Bohus, Sweden); and EPA-EE (> 99 %) and DHA-EE (> 99 %) were prepared in this laboratory.

The physical properties of C18-bonded silica are listed in Table 1. The surface coverage of C18-bonded silica and the particle size are provided by the producer, and the surface area and pore size distribution were determined by a Micromeritics ASAP2000 adsorption apparatus based on nitrogen adsorption. The pore size distribution of C18-bonded silica is also shown in Figure 1.

Apparatus. The apparatus for the adsorption measurements is illustrated in Figure 2. The constant volume system consists of a mixing cell 1 with a magnetic stirrer 2, a circulation pump 3, an adsorption column 4, and a UV detector. The mixing cell is equipped with a sapphire window through which the saturation of the solutes in SC−CO_2 can be monitored. A column of 4.6 mm I.D. × 50 mm is packed with C18-bonded silica. The UV detector was purchased from AllTech. The mixing cell and the adsorption column were located in a thermostat with a temper-

Table 3. Adsorption Data of EPA-EE and DHA-EE[a]

EPA-EE						DHA-EE					
318.15 K		328.15 K		338.15 K		318.15 K		328.15 K		338.15 K	
q	*y*	*q*	*y*	*q*	*y*	*q*	*y*	*q*	*y*	*q*	*y*
0.497 g·mL^{-1}						0.497 g·mL^{-1}					
0.015	0.509	0.013	0.59	0.012	0.63	0.01	0.21	0.009	0.25	0.007	0.333
0.044	1.56	0.040	1.72	0.035	1.90	0.019	0.47	0.017	0.55	0.016	0.59
0.080	4.54	0.080	4.54	0.063	5.17	0.034	0.91	0.031	0.99	0.027	1.17
0.117	5.29	0.106	5.69	0.093	6.21	0.059	1.94	0.053	2.16	0.048	2.35
0.173	6.41	0.163	6.76	0.149	7.30	0.082	3.05	0.076	3.28	0.064	3.75
0.275	6.86	0.252	7.71	0.226	8.72	0.091	3.71	0.083	4.00	0.076	4.29
0.618 g·mL^{-1}						0.098	4.21	0.092	4.47	0.083	4.81
0.011	0.177	0.008	0.26	0.008	0.273	0.167	5.57	0.158	5.92	0.146	6.37
0.021	0.745	0.019	0.78	0.015	0.922	0.251	6.29	0.239	6.77	0.225	7.33
0.025	1.49	0.023	1.54	0.021	1.61	0.618 g·mL^{-1}					
0.029	2.25	0.025	2.36	0.023	2.42	0.015	0.35	0.013	0.40	0.011	0.464
0.037	3.78	0.033	3.83	0.031	3.89	0.025	0.84	0.021	0.98	0.019	1.01
0.049	6.07	0.043	6.13	0.041	6.22	0.039	2.03	0.033	2.22	0.026	2.43
0.065	8.19	0.058	8.30	0.053	8.45	0.047	4.21	0.042	4.38	0.038	4.51
0.085	10.22	0.076	10.32	0.067	10.62	0.072	5.86	0.059	6.28	0.055	6.42
0.109	12.11	0.095	12.35	0.082	12.76	0.1	7.43	0.078	8.11	0.071	8.34
0.723 g·mL^{-1}						0.13	8.92	0.102	9.80	0.090	10.20
0.004	0.334	0.004	0.346	0.003	0.371	0.723 g·mL^{-1}					
0.011	0.891	0.011	0.899	0.011	0.906	0.007	0.5	0.006	0.54	0.006	0.549
0.019	2.19	0.018	2.21	0.017	2.24	0.014	1.02	0.011	1.09	0.010	1.12
0.024	3.55	0.023	3.55	0.021	3.61	0.026	2.09	0.024	2.16	0.021	2.24
0.027	4.96	0.025	5.02	0.024	5.04	0.036	3.92	0.033	3.99	0.032	4.03
0.032	6.32	0.029	6.39	0.027	6.44	0.042	5.85	0.039	5.93	0.038	5.96
0.033	7.78	0.032	7.81	0.030	7.87	0.053	9.06	0.05	9.13	0.048	9.20
0.035	9.23	0.034	9.26	0.032	9.32						

[a] (*q*/mmol·g^{-1}; *y*/10^{-4} mol·mol^{-1}).

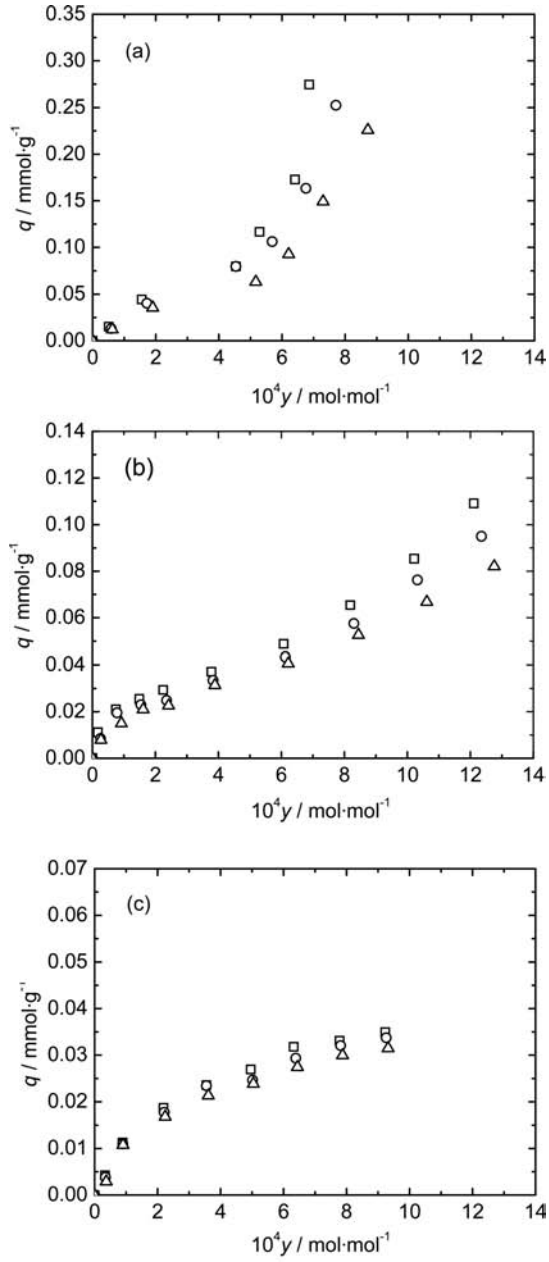

Figure 3. Adsorption isotherms of EPA-EE on C18-bonded silica at CO_2 densities of (a) 0.497 g·mL^{-1}, (b) 0.618 g·mL^{-1}, and (c) 0.723 g·mL^{-1}. □, 318.15 K; ○, 328.15 K; △, 338.15 K.

ature deviation of ± 0.1 K. The connect pipe outside the thermostat bath was wrapped in tubes with circulated water having the same temperature as the thermostat.

System Volume Determination. The system was first flushed using gaseous CO_2 for about 30 min to replace the air. After the temperature of thermostat became stable, CO_2 was then pumped into the system to a desired pressure. CO_2 was released out of the system slowly and bubbled through a sufficient quantity of KOH solution. After the CO_2 was completely released, the KOH solution was weighed. The mass of CO_2 in the system was obtained by the difference of the weight of the KOH solution after and before absorption. The density of CO_2 was calculated by the Span and Wagner equation of state[23] and is listed in Table 2. The system volume was then calculated according to the mass of CO_2 in the system and the density of CO_2. The system volume including the adsorption column was determined three times, the average value being 11.53 mL. The

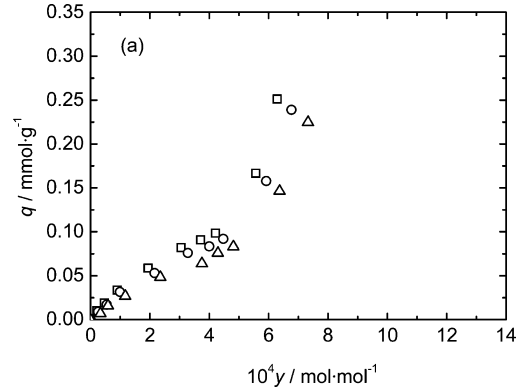

Figure 4. Adsorption isotherms of DHA-EE on C18-bonded silica at CO_2 densities of (a) 0.497 g·mL^{-1}, (b) 0.618 g·mL^{-1}, and (c) 0.723 g·mL^{-1}. □, 318.15 K; ○, 328.15 K; △, 338.15 K.

system volume without the column (while using a bypass tube) was determined to be 10.93 mL.

UV Detector Calibration. The bypass tube was connected to the system. CO_2 was compressed into the system to a desired value after the temperature of the thermostat became stable. The CO_2 flowed around the system by a circulation pump. A definite amount of EPA-EE or DHA-EE was injected into the six-port valve and then carried into the mixing cell and mixed by the flowing CO_2. After each injection, the solute concentration was calculated according to the injection volume and the total system volume. The corresponding UV absorbance of EPA-EE or DHA-EE was obtained from the detector. By the above procedures, the calibration curves between the UV absorbance and the solute concentration under different temperature and pressure conditions were obtained.

Adsorption Isotherm Determination. The bypass tube was replaced by the adsorption column, and the same procedures as the calibration mentioned above were repeated. After each injection, adsorption equilibrium was achieved when the detector response decreased to a constant value.

The amount of EPA-EE or DHA-EE adsorbed onto C18-bonded silica q can be calculated by

$$q = (\sum_{i=1}^{N} (m_i - VC_N)/M_1)/G \quad (1)$$

where m_i is the injected amount of the ith injection (mg); V is the volume of the constant volume system (mL); C_N is equilibrium concentration after the Nth injection (g·mL^{-1}) which can be obtained according to the calibration curves; M_1 is the molecular mass of solute (g·mol^{-1}); and G is the mass of C18-bonded silica in the adsorption column (g).

The equilibrium molecular fraction y of EPA-EE and DHA-EE in the supercritical CO_2 is calculated by

$$y = \frac{C_N}{M_1}\frac{M_2}{\rho} \quad (2)$$

where M_2 is the molecular mass of carbon dioxide (g·mol^{-1}) and ρ is the density of CO_2 (g·mL^{-1}).

Results and Discussion

The adsorption equilibrium data of EPA-EE and DHA-EE on C18-bonded silica from supercritical carbon dioxide at (318.15, 328.15, and 338.15) K were determined at CO_2 densities of (0.497, 0.618, and 0.723) g·mL^{-1}. The adsorption data are listed in Table 3. During the experiments, the mixed fluids in the mixing cell were all transparent by observing

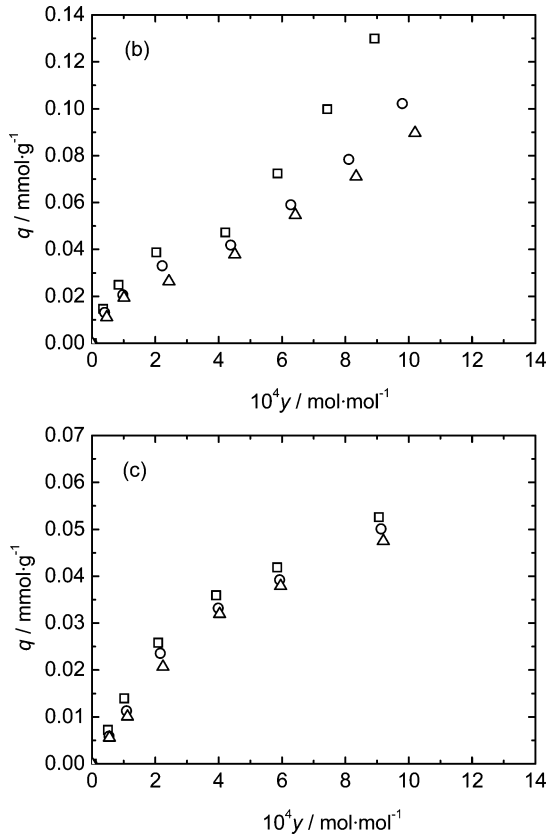

Figure 5. Adsorption data of EPA-EE at CO_2 densities of (a) 0.497 g·mL^{-1}, (b) 0.618 g·mL^{-1}, and (c) 0.723 g·mL^{-1} fitted by the BET equation. □, 318.15 K; ○, 328.15 K; △, 338.15 K; lines, BET equation.

through the window. Thus, the concentrations of all the experiments were below the saturation solubility of EPA-EE and DHA-EE in carbon dioxide.

Characteristics of the Adsorption Isotherms. Adsorption isotherms shown in Figures 3 and 4 indicate that the adsorption amount decreases while the temperature increases. This trend is in accordance with the basic principle of thermodynamics. In comparison to the adsorption from liquid solutions, the unique characteristic of adsorption from supercritical fluids is that the adsorption amount depends not only on the temperature and the bulk concentration but also on a new variable, the density of the supercritical fluid. It can be seen from Figures 3 and 4 that the adsorption amounts of EPA-EE or DHA-EE at a given temperature and bulk concentration decrease significantly as the carbon dioxide density increases. By interpolating the experimental data, the adsorption amount of solutes at three temperatures and different bulk concentrations can be obtained. For example, at 318.15 K and bulk concentration of EPA-EE of $6 \cdot 10^{-4}$ mol·mol^{-1}, the adsorption amount of EPA-EE under 0.497 g·mL^{-1} is 0.16 mmol·g^{-1}, whereas that under 0.723 g·mL^{-1} is 0.03 mmol·g^{-1}. This fact can be interpreted as follows. One factor is that with the increasing CO_2 density the number of CO_2 molecules around a solute molecule increases and the distance between the solute molecule and CO_2 molecules becomes less as well; consequently, the interaction between the solute and CO_2 molecules is enhanced significantly. As a result, the solubility of the solute in CO_2 increases, while the interaction between the solute and the adsorbent is weakened, which leads to a decrease of the adsorption amount. Another factor is that the reduced adsorption at higher CO_2 density is also due to the CO_2 adsorption competition for the adsorption sites. Figures 3 and 4 also indicate that with an increase of CO_2 density the

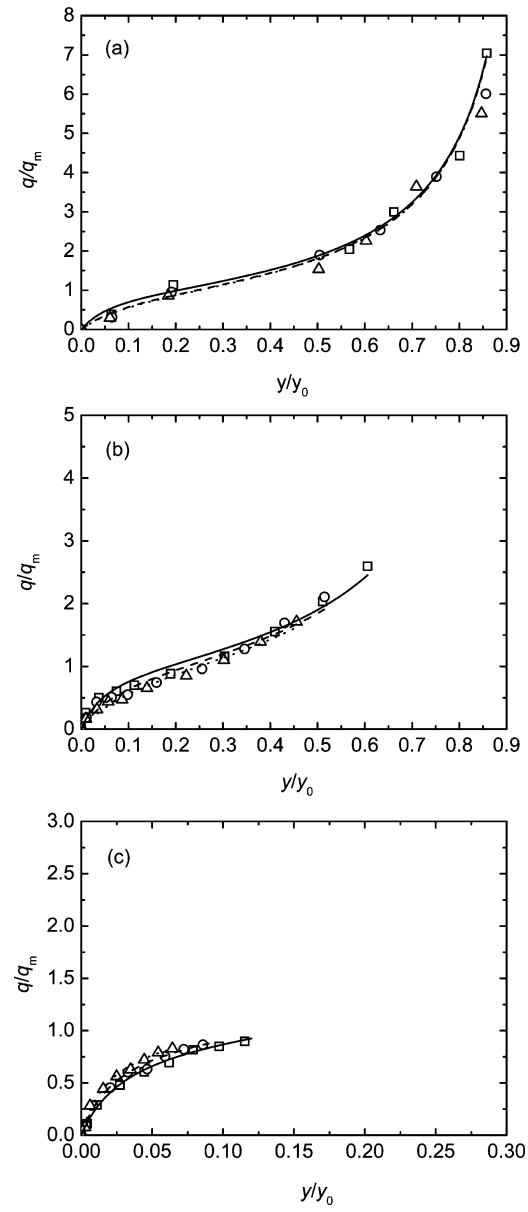

Figure 6. Adsorption data of DHA-EE at CO_2 densities of (a) 0.497 g·mL^{-1}, (b) 0.618 g·mL^{-1}, and (c) 0.723 g·mL^{-1} fitted by the BET equation. □, 318.15 K; ○, 328.15 K; △, 338.15 K; lines, BET equation.

Table 4. Estimated y_0

	$y_0/10^{-4}$ mol·mol^{-1}		
T/K	0.497 g·mL^{-1}	0.618 g·mL^{-1}	0.723 g·mL^{-1}
	EPA-EE		
318.15	8.0	20.0	80.0
328.15	9.0	24.0	108.0
338.15	10.3	28.0	145.0
	DHA-EE		
318.15	7.5	14.2	50.0
328.15	8.1	16.0	65.0
338.15	8.7	18.0	83.0

difference of adsorption amount between two temperatures becomes less.

Under the same conditions, the adsorption amount of DHA-EE is more than that of EPA-EE at the same equilibrium molecular fraction in CO_2, which is probably due to one more double bond of DHA-EE than EPA-EE.

Correlation of Adsorption Isotherms. Tan et al.[10,24] described the adsorption of toluene on activated carbon from supercritical

Table 5. Results of BET Correlation

		EPA-EE		DHA-EE	
ρ/g·mL^{-1}	T/K	q_m/mmol·g^{-1}	k/g·mmol^{-1}	q_m/mmol·g^{-1}	k/g·mmol^{-1}
0.497	318.15	0.039	15	0.048	18
	328.15	0.042	9.5	0.044	12
	338.15	0.041	9	0.040	10
0.618	318.15	0.042	19	0.046	16
	328.15	0.045	12	0.041	14
	338.15	0.048	9	0.040	13
0.723	318.15	0.039	32	0.054	17.5
	328.15	0.039	40	0.059	16.0
	338.15	0.038	50	0.063	17.0

carbon dioxide by the Langmuir and Toth models. Harikrishnan et al.[25] employed the Langmuir equation for modeling the adsorption breakthrough curves of ethylbenzene on activated carbon at supercritical conditions. Smirnova et al.[26] used the Langmuir equation to correlate the adsorption of Ketoprofen and Miconazole on hydrophilic and hydrophobic silica aerogels.

Figures 3 and 4 indicate that at a CO_2 density of 0.497 g·mL^{-1} and 0.618 g·mL^{-1} the adsorption isotherms of EPA-EE or DHA-EE are of typical type II isotherm character. At a CO_2 density of 0.723 g·mL^{-1}, the adsorption isotherms look like type I isotherms. Since the experimental data at a CO_2 density of 0.723 g·mL^{-1} are in the lower concentration range of the isotherm (much smaller than the solubility of the solute, refer to Figures 5(c) and 6(c)), the isotherms would be of type II character if data at higher concentration were determined. To our knowledge, type II isotherms at supercritical conditions are not found in the literature. Here, the classical BET multilayer adsorption model is employed to correlate the experimental data

$$\frac{q}{q_m} = \frac{kx}{(1-x)(1-x+kx)} \tag{3}$$

where q_m is the monolayer saturated capacity (mmol·g^{-1}); k is the BET constant; and x is the reduced concentration which is expressed by y/y_0 (y is the molecular fraction of solute in bulk phase, and y_0 is the solubility of solute in CO_2).

Solubilities y_0 under the conditions in this study are estimated from the equilibrium data of Bharath[27] by correlation of Chrastil's empirical equation[28]

$$y_0 = \rho^n \exp(a_1/T + a_2) \tag{4}$$

where constants a_1, a_2, and n are obtained by data fitting. The results are listed in Table 4.

Figures 5 and 6 indicate that the BET equation can fit the adsorption data quite well. The obtained parameters q_m and k are listed in Table 5. It is interesting to note that all the q_m values of EPA-EE under different temperatures and CO_2 densities are in the range of (0.038 to 0.048) mmol·g^{-1}, with an average of 0.041 mmol·g^{-1}. This conforms to the physical meaning of monolayer adsorption capacity which is defined as the amount of molecules adsorbed by the adsorption sites on the surface. Similar results hold for DHA-EE too. The monolayer adsorption amount of EPA-EE and DHA-EE on C18-bonded silica was converted to mmol·m^{-2} and compared with the values on silica gel from our previous work.[1] It was indicated that the monolayer adsorption amounts on both stationary phases are well consistent, and most of them are in the range of ($2.8 \cdot 10^{-7}$ to $3.9 \cdot 10^{-7}$) mol·m^{-2}.

The constant k can be expressed as $k \cong \exp[(Q_1 - Q_L)/RT]$, where Q_1 and Q_L are interaction energies between the adsorbate molecules and the adsorbent surface and between adsorbate and adsorbate molecules, respectively. So, Q_1 is the heat of adsorption and Q_L is the heat of evaporation. As shown in Table 5, at CO_2 densities of 0.497 g·mL^{-1} and 0.618 g·mL^{-1}, the value of k decreases with temperature, which indicates that Q_1 is larger than Q_L; on the contrary, at CO_2 density of 0.723 g·mL^{-1}, the k value increases with temperature, which indicates

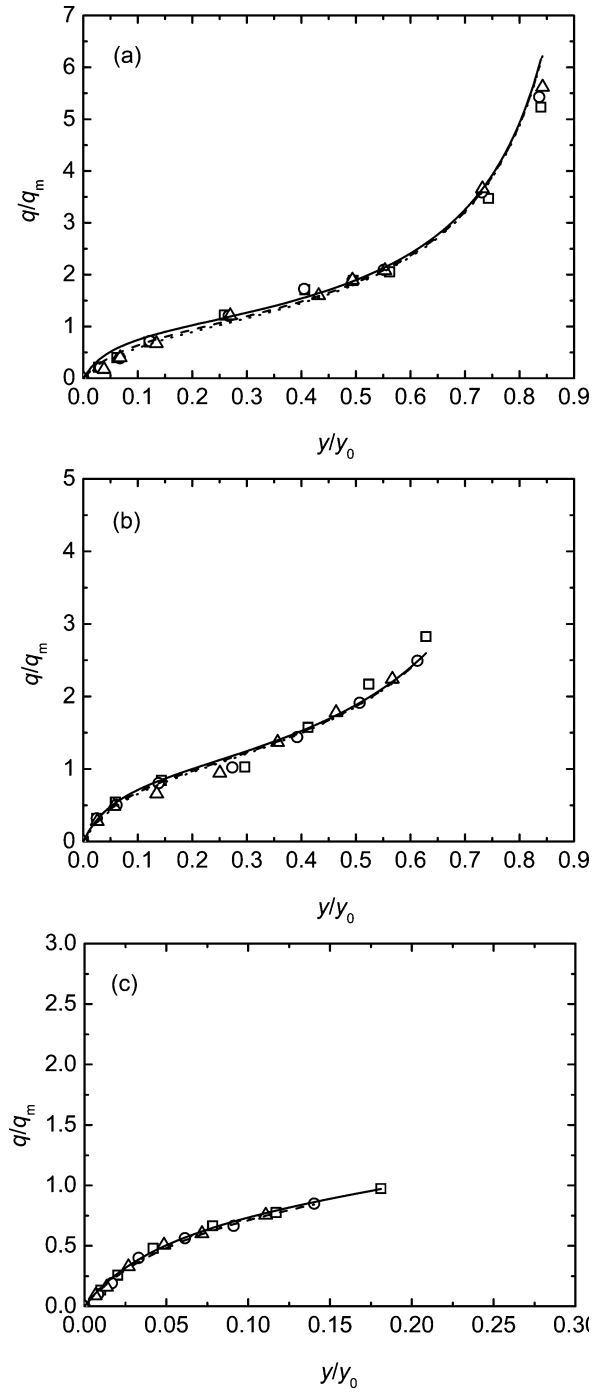

Figure 7. Comparison of the adsorption isotherms of (a) EPA-EE and (b) DHA-EE on C18-bonded silica at different densities and temperatures. ■, 0.497 g·mL^{-1}, 318.15 K; ●, 0.497 g·mL^{-1}, 328.15 K; ▲, 0.497 g·mL^{-1}, 338.15 K; □, 0.618 g·mL^{-1}, 318.15 K; ○, 0.618 g·mL^{-1}, 328.15 K; △, 0.618 g·mL^{-1}, 338.15 K; +, 0.723 g·mL^{-1}, 318.15 K; ×, 0.723 g·mL^{-1}, 328.15 K; −, 0.723 g·mL^{-1}, 338.15 K. Solid lines in (a) and (b) are the same.

Table 6. Physical Properties and Estimated σ of EPA-EE and DHA-EE

	T_c (K)	P_c (Mpa)	ω	σ (nm)
EPA-EE	833.8	1.181	1.013	0.94
DHA-EE	867.1	1.102	0.990	0.98

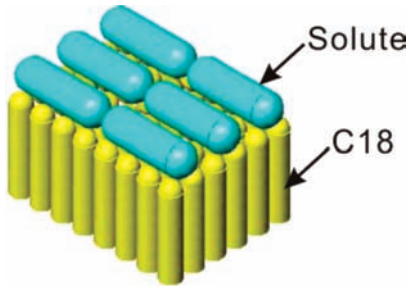

Figure 8. Packing model of EPA-EE or DHA-EE molecules on C18-bonded silica.

that Q_1 is smaller than Q_L. Figures 5 and 6 also show that when the adsorption data are plotted in q/q_m vs y/y_0 the adsorption isotherms at different temperatures almost coincide to a general curve. Unfortunately, because of the limited range of the UV detector, the determined y/y_0 at a CO_2 density of 0.723 g·mL^{-1} are restricted in the y/y_0 range of 0 to 0.2. Moreover, it was found that if all the adsorption data of EPA-EE and DHA-EE are plotted together in q/q_m vs y/y_0, respectively, a general characteristic adsorption curve is obtained, as shown in Figure 7. A similar result was published for the adsorption of aliphatic acid analogues on activated carbon from aqueous solution.[29] Whether this result is a general property for other solute−supercritical fluid systems, it is a problem deserving of further attention.

The Lennard-Jones molecular dynamic diameters σ of EPA-EE and DHA-EE can be estimated by[30]

$$\sigma\left(\frac{P_c}{T_c}\right)^{1/3} = 2.3351 - 0.087\omega \quad (5)$$

where P_c is the critical pressure (MPa); T_c is the critical temperature (K); and ω is the eccentric factor. The estimated results are listed in Table 6.

The calculated σ values of EPA-EE and DHA-EE molecules are close to that of the bonded C18 which is about 0.9 nm. Suppose the long chain axis of the adsorbed EPA-EE and DHA-EE molecules was perpendicular to the C18 surface, then the monolayer adsorption saturated capacity q_m can be calculated as follows

$$q_m = A\theta \quad (6)$$

where A is the surface area, m^2·g^{-1}, and θ is the surface coverage, μmol·m^{-2}. q_m of EPA-EE and DHA-EE would be about 0.46 mmol·g^{-1}.

If the adsorbed EPA-EE and DHA-EE molecules lie with their chain axis parallel to the bonded C18 surface as shown in Figure 8, which results in the lowest potential of the adsorbed molecules, then q_m can be calculated as follows

$$q_m = \frac{A}{N_A \sigma L} \quad (7)$$

where L is the axial length of the long-chain solute, about 4.6 nm, and N_A is the Avogadro constant. The calculated q_m is 0.0527 mmol·g^{-1}, which is in the range of the q_m obtained by correlation, (0.04 to 0.05) mmol·g^{-1}. This implies that the C18 surface is initially covered by a monolayer of EPA-EE and DHA-EE molecules that lay on the C18 surface, and then the succeeding layers of the solutes are formed.

Heat of Adsorption. The experiment in this work is performed under isochoric conditions, so the adsorption heat at different adsorption amounts is expressed by the partial molecular internal

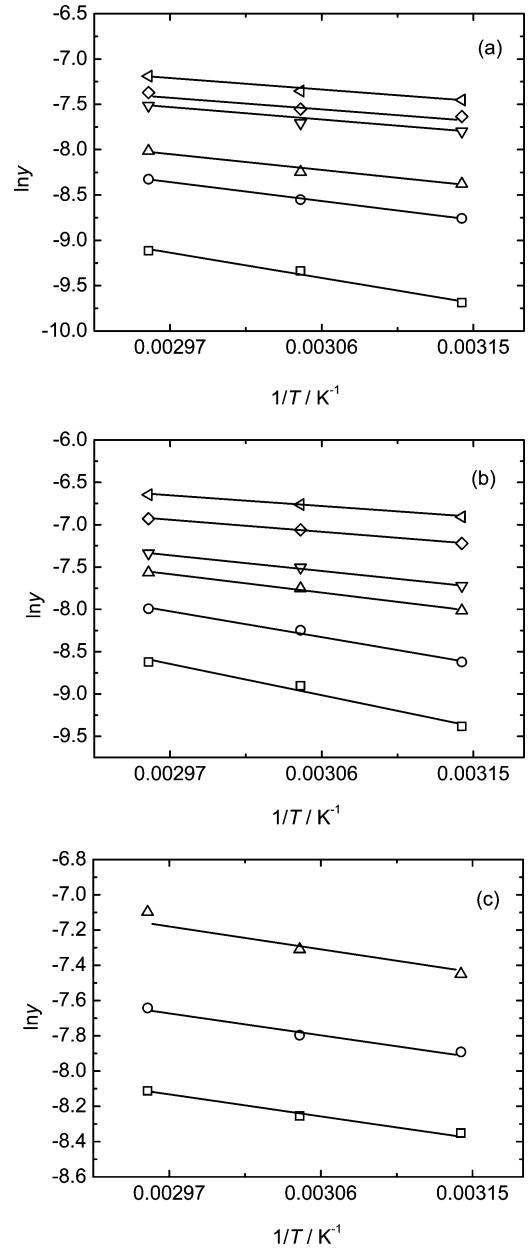

Figure 9. Adsorption isosteres of EPA-EE at densities of (a) 0.497 g·mL^{-1}, (b) 0.618 g·mL^{-1}, and (c) 0.723 g·mL^{-1}. In Figure (a): □, 0.025 mmol·g^{-1}; ○, 0.040 mmol·g^{-1}; △, 0.050 mmol·g^{-1}; ▽, 0.080 mmol·g^{-1}; ◇, 0.100 mmol·g^{-1}; open triangle pointing left, 0.150 mmol·g^{-1}. In Figure (b): □, 0.020 mmol·g^{-1}; ○, 0.030 mmol·g^{-1}; △, 0.040 mmol·g^{-1}; ▽, 0.046 mmol·g^{-1}; ◇, 0.060 mmol·g^{-1}; open triangle pointing left, 0.080 mmol·g^{-1}. In Figure (c): □, 0.020 mmol·g^{-1}; ○, 0.025 mmol·g^{-1}; △, 0.030 mmol·g^{-1}.

energy changes between the adsorbent and supercritical fluid and can be represented by[24]

$$\left(\frac{\partial \ln y}{\partial T}\right)_{\rho,q} = \frac{Q}{RT^2} \quad (8)$$

where Q is the isosteric heat of adsorption (kJ·mol^{-1}). Because the experimental data were not determined at constant adsorbed amounts, the constant adsorbed amounts in Figures 9 and 10 were obtained from the BET correlation.

Within the temperature range of this work, Q can be regarded as independent of temperature. After integration, the following equation is obtained

$$\ln y = -\frac{Q}{RT} + B \tag{9}$$

where B is a constant.

Figures 9 and 10 show the isosteres of EPA-EE and DHA-EE, respectively. The isosteric heat of adsorption Q which can be calculated from the slopes of the lines is plotted against q/q_m in Figure 11. It can be seen that the isosteric heat of adsorption at low surface coverage is large and then it decays exponentially with q/q_m, which is consistent with the literatrue.[31] At q/q_m around 1.8, the curve levels off because the adsorption between solute molecules dominates and the heat released by condensation of the solute keeps constant. Furthermore, the adsorption heat is related to CO_2 density. The adsorption heat is the energy change when the solute molecule replaces the CO_2 molecule on C18-bonded silica and then is adsorbed onto the surface; therefore, with greater CO_2 density, the energy for the solute molecule to escape from the bulk phase would be greater, and the energy for replacing the CO_2 on the surface would be greater as well, which leads to the decrease of adsorption heat.

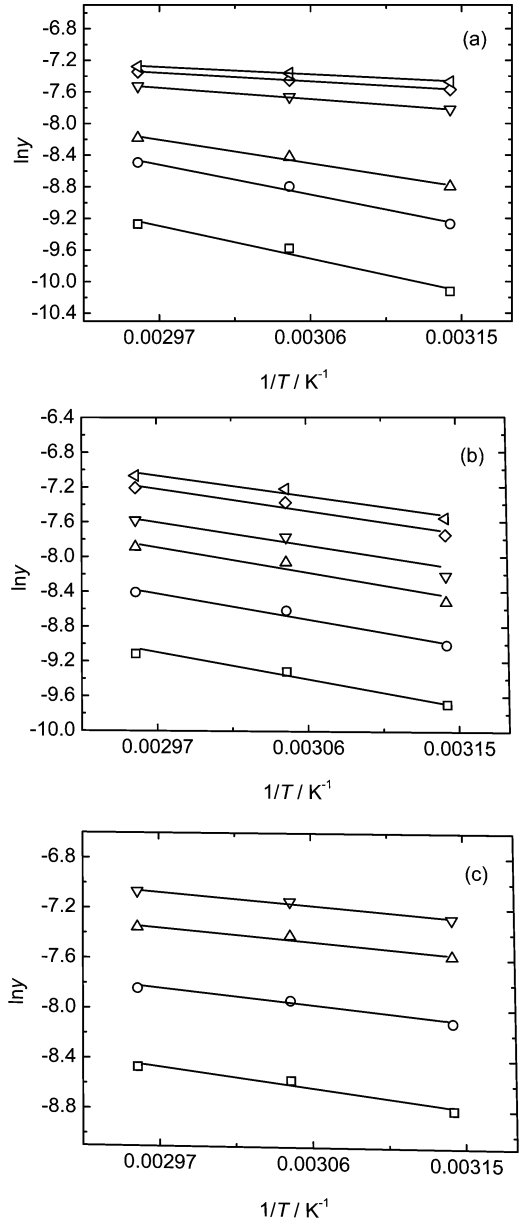

Figure 10. Adsorption isosteres of DHA-EE at densities of (a) 0.497 g·mL^{-1}, (b) 0.618 g·mL^{-1}, and (c) 0.723 g·mL^{-1}. In Figure (a): □, 0.025 mmol·g^{-1}; ○, 0.040 mmol·g^{-1}; △, 0.050 mmol·g^{-1}; ▽, 0.100 mmol·g^{-1}; ◇, 0.150 mmol·g^{-1}; open triangle pointing left, 0.200 mmol·g^{-1}. In Figure (b): □, 0.020 mmol·g^{-1}; ○, 0.030 mmol·g^{-1}; △, 0.040 mmol·g^{-1}; ▽, 0.046 mmol·g^{-1}; ◇, 0.060 mmol·g^{-1}; open triangle pointing left, 0.070 mmol·g^{-1}. In Figure (c): □, 0.020 mmol·g^{-1}; ○, 0.030 mmol·g^{-1}; △, 0.040 mmol·g^{-1}; ▽, 0.046 mmol·g^{-1}.

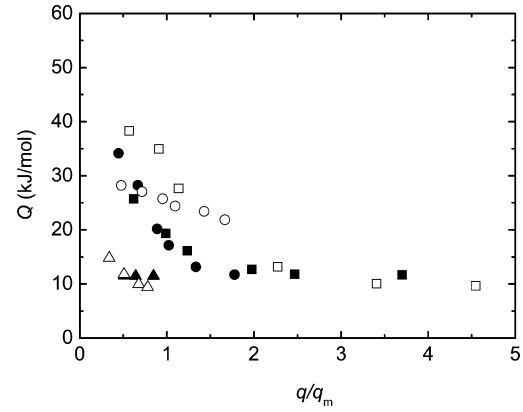

Figure 11. Dependence of Q for EPA-EE and DHA-EE on q/q_m at different densities. ■ and □, 0.497 g·mL^{-1}; ● and ○, 0.618 g·mL^{-1}; ▲ and △, 0.723 g·mL^{-1}; closed symbols, EPA-EE; open symbols, DHA-EE.

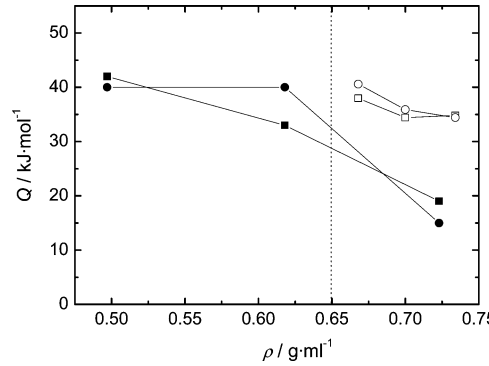

Figure 12. Comparison of the heat of adsorption on C18-bonded silica and silica gel. ■, EPA-EE on C18-bonded silica; ●, DHA-EE on C18-bonded silica; □, EPA-EE on silica gel; ○, DHA-EE on silica gel.

The infinite dilution heat of adsorption of EPA-EE and DHA-EE on C18-bonded silica was obtained by trend extrapolation using the data in Figure 11. These values are compared with the previous data on silica gel.[1] As shown in Figure 12, the heat of adsorption on C18-bonded silica is far greater than the value on silica gel when CO_2 density is higher than 0.650 g·mL^{-1}. This may be due to the stronger interaction between the hydroxyl of silica gel and adsorbate than that between C18 and adsorbate.

Conclusions

(1) The adsorption amount of solute (EPA-EE and DHA-EE) on C18-bonded silica from supercritical carbon dioxide depends not only on the temperature and the solute concentration in bulk but also on the CO_2 density significantly. (2) The adsorption isotherms of EPA-EE and DHA-EE from supercritical carbon dioxide are of type II isotherm character. The BET model can fit the adsorption data well. (3) When the adsorption data are plotted by the reduced parameters q/q_m vs y/y_0, all the adsorption isotherms almost coincide to a general characteristic curve. The effect of the solubility of the solute and the CO_2 density on the adsorption amount can be simplified by using the reduced parameter. (4) Adsorption of EPA-EE and DHA-EE on C18-bonded silica is an exothermic process. The

adsorption amount and CO_2 density are the main factors affecting the adsorption heat.

Literature Cited

(1) Han, Y. S.; Yang, Y. W.; Wu, P. D. Adsorption Equilibria of *cis*-5,8,11,14,17-Eicosapentaenoic Acid Ethyl Ester and *cis*-4,7,10,13,16,19-Docosahexaenoic Acid Ethyl Ester from Supercritical Carbon Dioxide on Silica Gel. *J. Chem. Eng. Data* **2008**, *53*, 16–19.

(2) Nilsson, W. B.; Gauglitz, E. J.; Hudson, J. K.; Stout, V. F.; Spinelli, J. Fractionation of menhaden oil ethyl esters using supercritical fluid CO_2. *JAOCS* **1988**, *65*, 109–117.

(3) Perrut, M. Purification of polyunsaturated fatty acid (EPA and DHA) ethyl esters by preparative high performance liquid chromatography. *LC-GC* **1988**, *6*, 914–920.

(4) Berger, C.; Jusforgues, P.; Perrut, M. Purification of unsaturated fatty acid esters by preparative supercritical fluid chromatography, In *Proceedings of the 1st International Symposium on Supercritical Fluids*, Nice, 1988; pp 397−404.

(5) Alkio, M.; Gonzalez, C.; Jäntti, M.; Aaltonen, O. Purification of polyunsaturated fatty acid esters from tuna oil with supercritical fluid chromatography. *JAOCS* **2000**, *77*, 315–321.

(6) Yamaguchi, M.; Kadota, Y.; Tanaka, I.; Ohtsu, Y. New separation method of high-purity DHA by supercritical fluid chromatography. *J. Jpn. Oil Chem. Soc.* **1999**, *48*, 1169–1176.

(7) Pettinello, G.; Bertucco, A.; Pollado, P.; Stassi, A. Production of EPA enriched mixtures by supercritical fluid chromatography: from the laboratory scale to the pilot plant. *J. Supercrit. Fluids* **2000**, *19*, 51–60.

(8) Yang, Y. W.; Wu, C. J.; Wang, X. D.; Huang, M.; Ren, Q. L. Purification of EPA-EE and DHA-EE with supercritical fluid chromatography. *J. Chem. Eng. Chinese Univ.* **2004**, *18*, 293–296.

(9) Lembke, P. Process-scale SFC: a feasibility study, in *Proceedings of the 7th International Symposium on Supercritical Fluid Chromatography and Extraction*, Indianapolis, 1996.

(10) Tan, C. S.; Liou, D. C. Adsorption equilibrium of toluene from supercritical carbon dioxide on activated carbon. *Ind. Eng. Chem. Res.* **1990**, *29*, 1412–1415.

(11) Tan, C. S.; Liou, D. C. Desorption of ethyl acetate from activated carbon by supercritical carbon dioxide. *Ind. Eng. Chem. Res.* **1988**, *27*, 988–991.

(12) Buβ, V. Präparative Chromatographie mit überkritischen Fluiden am Beispiel einer Vitaminreinigung. Dissertation, Technische Universität Hamburg-Harburg, Hamburg, 2002.

(13) Buβ, V.; Johannsen, M.; Brunner, G. Preparative supercritical fluid chromatography in elution mode, in *Proceeding of the Second International Meeting on High Pressure Chemical Engineering*, Hamburg, Germany, Germany, March 7−9, 2001.

(14) Bolten, D.; Johannsen, M. Influence of 2-propanol on adsorption equilibria of α- and β-tocopherol from supercritical carbon dioxide on silica gel. *J. Chem. Eng. Data* **2006**, *51*, 2132–2137.

(15) Lubbert, M.; Brunner, G.; Johannsen, M. Adsorption equilibria of alpha- and delta-tocopherol from supercritical mixtures of carbon dioxide and 2-propanol onto silica by means of perturbation chromatography. *J. Supercrit. Fluids* **2007**, *42*, 180–188.

(16) Sato, M.; Goto, M.; Kodama, A.; Hirose, T. New fractionation process for citrus oil by pressure swing adsorption in supercritical carbon dioxide. *Chem. Eng. Sci.* **1998**, *53*, 4095–4104.

(17) Reverchon, E.; Lamberti, G.; Subra, P. Modelling and simulation of the supercritical adsorption of complex terpene mixtures. *Chem. Eng. Sci.* **1998**, *53*, 3537–3544.

(18) Subra, P.; Bancel, A. V.; Reeverchon, E. Breakthrough curves and adsorption isotherms of terpene mixtures in supercritical carbon dioxide. *J. Supercrit. Fluids* **1998**, *12*, 43–57.

(19) Lucas, S.; Cocero, M. J.; Zetzl, C.; Brunner, G. Adsorption isotherms for ethylacetate and furfural on activated carbon from supercritical carbon dioxide. *Fluid Phase Equilib.* **2004**, *219*, 171–179.

(20) Kikic, I.; Alessi, P.; Cortesi, A. An experimental study of supercritical adsorption equilibria salicylic acid on activated carbon. *Fluid Phase Equilib.* **1996**, *117*, 304–311.

(21) Gregorowicz, J. Adsorption of eicosane and 1,2-hexanediol from supercritical carbon dioxide on activated carbon and chromosorb. *Fluid Phase Equilib.* **2005**, *238*, 142–148.

(22) Skerget, M.; Knez, Z. Supercritical fluid adsorption and desorption of lipids on various adsorbents. *Acta Chim. Slov.* **2007**, *54*, 688–692.

(23) Span, R.; Wagner, W. A new equation of state for carbon dioxide covering the fluid region from the triple-point temperature to 1100K at pressures up to 800 MPa. *J. Phys. Chem. Ref. Data* **1996**, *25*, 1509–1596.

(24) Lai, C. C.; Tan, C. S. Heat effect for toluene adsorption on activated carbon from superciritcal carbon dioxide. *Fluid Phase Equilib.* **1995**, *111*, 127–141.

(25) Harikrishnan, R.; Srinivasan, M. P.; Ching, C. B. Adsorption of ethyl benzene on activated carbon from supercritical CO_2. *AIChE J.* **1998**, *44*, 2620–2627.

(26) Smirnova, I.; Mamic, J.; Arlt, W. Adsorption of drugs on silica aerogels. *Langmuir* **2003**, *19*, 8521–8525.

(27) Bharath, R.; Inomata, H.; Arai, K. Vapor-liquid equilibria for binary mixtures of carbon dioxide and fatty acid ethyl esters. *Fluid Phase Equilib.* **1989**, *50*, 315–327.

(28) Chrastil, J. Solubility of solids and liquids in supercritical gases. *J. Phys. Chem.* **1982**, *86*, 3016–3021.

(29) Hansen, S. R.; Craig, R. P. The adsorption of aliphatic alcohols and acids from aqueous solutions by non-porous carbon. *J. Phys. Chem.* **1954**, *58*, 211–15.

(30) Reid, R. C.; Prausnitz, J. M.; Sherwood, T. K. *The properties of gases and liquids,* 3rd ed.;McGraw-Hill: Singapore, 1977.

(31) Oldenkamp, R. D.; Houghton, G. Isosteric Heats of Adsorption of Isobutylene on Activated Alumina. *J. Phys. Chem.* **1963**, *67*, 303–306.

Received for review December 30, 2008. Accepted June 19, 2009. The authors are grateful for the financial support from the Ministry of Science and Technology of the People's Republic of China (project Nos. 2006BAD27B03 and 2007AA100404) and the National Natural Science Foundation of China (No. 20676112).

JE801003D